JREE: Vol. 9, No. 1, (Winter 2022) 53-62

Journal of Renewable Energy and Environment

Journal Homepage: www.jree.ir

Materials and Energy Research Center

MERC

Research Article

The Effect of Roof Integrated Photovoltaic (RIPV) on Building Indoor Air in African Tropical Climate

Aloys Martial Ekoe A. Akata *

Department of Physics, Faculty of Science, University of Douala, P. O. Box: 2701, Douala, Cameroon.

PAPER INFO

Paper history:
Received: 28 November 2020
Revised in revised form: 21 February 2021
Scientific Accepted: 12 March 2021
Published: 21 November 2021

Keywords:
Building Integrated Photovoltaic (BIPV),
Thermal Comfort,
Heat Transfer,
Indoor Air Temperature,
Photovoltaic,
Solar Roof

ABSTRACT

Photovoltaic energy has the potential to become one of the major energy sources used in the households in the tropical region of Africa, where the solar radiation intensity is abundant and almost constant over the year. Solar photovoltaic systems present many advantages when they are integrated in the building structure envelope and have a significant influence on the indoor air temperature of dwelling buildings due to the thermal resistance modification. In this paper, a simplified model of the photovoltaic system integrated on the roof of a residential building according to the building construction customs and materials has been designed and modeled. The heat transfer is studied in several situations: with and without a Building Integrated Photovoltaic (BIPV) system and for a building with and without false ceiling. The BIPV system installed over an effective area of 35 m^2 increases the building indoor air temperature of approximately 5 °C which is corrected by the heat insulation optimization of the false ceiling made up with building local materials. The final indoor air temperature obtained is in good agreement with the ASHRAE standards and can, therefore, be applied to tropical regions.

https://doi.org/10.30501/jree.2021.259138.1166

1. INTRODUCTION

Tropical countries are situated between latitude +15 °C and -15 °C and are extended to the warm and humid zones of Central Africa, Central America, southern Asia, and northern South America; temperatures range between 24 and 33 °C and the humidity may be frequently between 60 and 100 %. The tropical climate is expanded on to three different continents: Oceania, Asia, and Africa. Hence, the energy consumption of a building in a tropical climate of each of these continents is not automatically identical, but is closely related to the geographical location of the country. In Australia, air conditioning (space heating and/or cooling) is the main source of energy consumption (35 %) followed by residential appliances (24 %), water heating (23 %), and lighting (7 %) [1]. As Australia is located in the tropical region of Oceania where in the south regions of Australia, the winter is mild and the summer hot and the temperatures oscillate between 10 and 21 °C. Hence, the comfort resumes to increase the indoor air temperature. An opposite perception of the thermal comfort exits in Malaysia and other East Asia countries, where the comfort resumes to lower the indoor air temperature. Concerning the country of Cameroon, to meet the needs of an increasing energy demand remains a mission accomplished to a lesser extent; despite setting up new energy sources such as power gas stations and steam-generating stations, the cover of the national territory in electric power still remains low enough, about less than 50 % and 10 % in urban and rural areas, respectively. This is due to the great distance between the production and consumption sites, hence inducing a significant energy loss during its transport representing almost 30 % of the electric power produced [2]. From the analysis made on tropical countries, a focus can be made on the two following problems: 1) Reducing the energy consumption of the residential building used for space cooling; 2) Reducing the dependence of traditional (non-renewable) energy sources. A common solution to these two problems can be found: the use of renewable energy.

1.1. Photovoltaic systems

Renewable energies refer to energy sources that are renewed quickly enough to be considered as inexhaustible on the human scale. There are many types of renewable energies: solar energy, wind energy, biomass energy, hydraulic energy, etc. As their use has a negligible impact on our environment, the conception of a sustainable development passes through an increasing implementation of renewable energy sources. Among the renewable energy sources, solar energy has the capacity to become one of the major energy sources in tropical climates. Solar energy should therefore constitute the real source of electrical production and thermal energy in all sectors, particularly the residential sector because of its on-site production. Indeed, Chen et al. [3] claimed that from incident

*Corresponding Author's Email: ekoealoys@yahoo.fr (A.M. Ekoe A. Akata)
URL: https://www.jree.ir/article_140549.html

Please cite this article as: Ekoe A. Akata, A.M., "The effect of roof integrated photovoltaic (RIPV) on building indoor air in African tropical climate", ***Journal of Renewable Energy and Environment (JREE)***, Vol. 9, No. 1, (2022), 53-62. (https://doi.org/10.30501/jree.2021.259138.1166).

solar radiation, measured in the city of Brazl, in the period of 2007 to 2012, they obtained an average power generation of 11.0 kWh/day and efficiency of the modules in the order of 12.6 %.

In the past, it was common to lay PV panels on the roof of the already designed building; this concept is called Building Applied Photovoltaic (BAPV) [4]. This solution was not very adequate as it was necessary to spend both for the roof and PV panels; in addition to that, the increasing temperature of the PV panels leads to a reduction in their efficiency [5]. All that contributed to the elaboration of the BIPV concept, i.e., the solar photovoltaic system was integrated in the structure of the building envelope. PV panels, therefore, replace a part of the materials used in the construction of the building roof [6]. It is also possible to integrate photovoltaic to the walls. This concept enables to make savings on building materials and space integration. To maintain the PV panels' temperature to a value enabling their optimal functioning, the idea of the hybrid PV/T solar collector was put forward. Chow et al. [7] proposed an aluminum-alloy flat-box type PVT collector using water as the coolant fluid and the fin efficiency approached unity, leading to the thermal efficiency of 57.4 %. Ekoe et al. [8] proposed as solution the setting-up of fins on the back sheet of the photovoltaic module of the Building Integrated Semitransparent PhotoVoltaic Thermal system (BISPVT) system; the heat extracted from the air circulating in the rectangular duct at the back sheet of the PV module can be used to warm the building indoor air temperature. An annual production of 76.66 kWh of thermal energy at an overall thermal efficiency rate of 56.07 % is obtained with a system area of 36 m^2. They thus arrived to the same conclusions as Maturi et al. [9] who got the same results experimentally. The so-extracted energy can be used in electric power production and also, the thermal energy can be used to warm the building indoor air temperature and to produce hot domestic water. The so-used sensor is called a PhotoVoltaic Thermal (PV/T) sensor. This concept developed by the authors of [10-12] has shown its effectiveness. Even though energy production through PV systems is important, the indoor air quality of the building is another aspect that should be considered carefully.

1.2. The effect of PV on thermal comfort of a building

The results obtained from various researches show that proper ventilation and the absence of airtight devices, installed to reduce energy consumption, favor the indoor/outdoor air exchange and thus contribute to the enhancement of Indoor Air Quality. Several studies have been carried out to quantify the impact of a solar photovoltaic system on the building indoor air temperature and humidity (Iath). Benradouane et al. [13] designed and adapted a thermo-solar house on the site of Tlemcen, Algeria which allows a significant storage of the heat coming from solar rays in order to do cancel the use of auxiliary energy sources. They found that South, East, and West orientations facilitated obtaining good results. Obeng et al. [14] conducted a study in the rural households of Ghana as they depended mainly on kerosene lanterns for lighting after sunset. They compared households with and without solar PV in off-grid rural Ghana and came to two major conclusions: firstly, the proportion of household members being affected by indoor smoke from kerosene lanterns could be reduced by 50 % thanks to the use of solar PV lighting. Secondly, solar PV lighting can probably reduce the proportion of household members who get blackened nostrils from soot associated with kerosene lanterns by approximately a third. These conclusions reflect the reality as during their operation, PV panels produce no air pollution, hazardous waste, or noise.

In order to analyze the comfort aspect (thermal and lighting aspects) of PV modules and PV systems for vertical integration, Lopez et al. [15] presented a work dealing with the specific design of the test facility and the methodology employed for BIPV reproducing the internal conditions of a real building. The temperatures they obtained during the conducted experiments never went above the interval 23 °C and 27 °C as specified by the "European Adaptive Standard", EN 15251:2007-08, but were sometimes below the minimum specified value. Green buildings not only provide an improved worker productivity and work quality as a result of a more comfortable office environment, but also an improved public health resulting from reduced indoor air pollution. Wen I-Jyh et al. [16] conducted a study where they designed a ventilated BIPV with a double roof structure in order to introduce indoor ventilation and also provide itself with environmental control. From the results obtained, they concluded that both ventilated BIPV designs proposed in this study can provide appropriate indoor thermal environments.

Two other research works deserve to be mentioned. The first one is the study done by Dominguez et al. [17] who quantified the indirect benefits of a photovoltaic roof for the insulation of the cement roof of the Powell Structural systems Laboratory (PoSL) at the University of San Diego, California. The heat flux modeling of theirs has shown a significant reduction in daytime roof heat flux under the PV array, while at night, the conditions reversed. They have thus obtained a 5.9 $kWhm^{-2}$ (or 38 %) reduction in annual cooling load. The second one comes from Ekoe et al. [18] who studied the influence of the integration of solar systems in the envelope structure of the building on the indoor air temperatures and humidity of a building under the tropical climatic conditions of Yaoundé, Cameroon. They have found that BIPV increases the building's indoor air temperature by 4°C, when compared to a building of the same size without PV integrated. They have also shown that a judicious choice of the building materials and the orientation of the building allow minimizing that temperature difference. Among these two options, the choice of the building materials is the solution accessible to everyone.

1.3. False ceiling in tropical regions

Various techniques can be used to improve the thermal comfort of a building, namely the HVAC system, energy production, and the elements of the building's envelope. The appropriate use of such techniques depends on the typology of the building, the construction habits, and climatic conditions of the area. The studies on the rational use of energy in buildings located in tropical regions have been focused on the reduction of energy consumption in buildings through the optimum utilization of the thermal insulation of the envelope. In the case of Cameroon, the main source of energy consumption is air conditioning followed by lighting. Therefore, the thermal comfort resumes to the lowering of the indoor air temperature. This can be efficiently achieved by increasing the thermal inertia of the building through the use of a false ceiling.

In the Cameroonian context, the false ceiling is a solid and horizontal surface that closes up a living room parallel to the

floor. It is made up of local materials, especially wood. The false ceiling is used for decoration of the building and the hiding of electric cables. It can also be used for the installation of ceiling fans; people are used to employ ceiling light in order to obtain a better lighting than when the lamps are fixed on the wall. The space between the false ceiling and the roof is referred to as the dead space. The air contained in the dead space greatly influences the indoor comfort. Indeed, a great part of the heat gained by the building is done through the elements of the roof. Normally, almost all the heat is transferred to the building, resulting in indoor thermal discomfort. Hence, the use of the false ceiling increases the thermal inertial of the building, reduces the thermal heat transferred in the leaving space, and produces more comfortable conditions for the occupants of the building. As wood is among the local building materials, its use as false ceiling is the ideal solution to obtain comfortable indoor air conditions.

The authors [19] established a transient 1-D model to study the role of such a ceiling in the reduction of the ambient indoor air temperature. The use of false ceiling only without reflector sheet reduced the heat gain introduced to space for a whole day by 66.8 %, while the use of a false ceiling with reflector sheet increased the reduction percentage of heat gained from the concrete roof to be 81.6 % during the same period. However, the building that they have studied did not have PV panels, the roof was made up of concrete and the temperature of the building was controlled.

Basically, the roof of the building can be described as the upper part of the envelope which protects the building against the climatic elements that could be harmful to the inhabitants of the building. The climatic elements include sun light, rain, birds excrement, etc. The materials used in the roof construction vary from one geographical area to another. In the tropical sub-Saharan African climate and specifically in urban zones, the roofs are mainly made up of Aluminum due to its reflecting properties. The Aluminum sheets are fixed with wooden slats to prevent them from getting carried away by wind. This construction style is reproduced in almost all the buildings in urban areas. Concerning buildings with many floors, such roof is used to cover the last floor of the building. However, due to the conducting properties of Aluminum, a great part of the heat absorbed by the roof is transferred to the floor of the building. To reduce the quantity of heat transferred to the floor of the building, the simple roof, i.e., the roof made only of steel, can be completed by the addition of the false ceiling in order to provide pleasant indoor conditions to the occupants of the building. In this paper, the simple roof refers to a roof made up of only Aluminum, while the term roof indicates the unit made up of the Aluminum, the dead space, and the false ceiling.

Our study comes after all those studies and focuses on two important aspects: the presence or not of false ceiling and PV panels on the roof of the building, and their influence on the indoor air temperature and humidity. Modeling of the roof heat flow through the different elements of the envelope of the building has been done for a tropical climate of Cameroon in order to characterize the comfort conditions inside the building according to those aspects.

2. PROBLEM IDENTIFICATION

In Cameroon, the energy used for building lighting represents almost 20 % of the energy consumption in the residential sector and almost 25 % in offices and commercial buildings. The electric power produced by the BIPV system could be used for the lighting of the building, the corridor, and the outside light; however, this paper does not focus on the electric power which can be produced by the BIPV system. The building under consideration is situated in Yaoundé at 4.051N, 9.768E, and a site altitude of 103 m. The size of the building is 15 m × 11 m with an average height of 6.5 m. The roof is south oriented. The building is insulated by a layer of sand, cement, and paint. The Photovoltaic system is integrated at the roof top covering an effective area of 450 m^2. The BIPV system is made of polycrystalline PV modules. The BIPV system, area of 35 m^2, and made up of 20 PV modules and peak power of 4 kWh is oriented in opposite direction with the wind in order to optimize the natural convection. Moreover, the space left between the false ceiling and the roof (dead space) also takes part in the temperature lowering of the ambient air of the building. Thus, the height of the false ceiling can be chosen as 0.75 m with a thickness of 4 mm, depending on the other dimensions of the building.

3. MODELLING OF ROOF PV

As envisaged in the summary and the introduction, several cases will be studied, as shown in Figure 1:

1. The building does not have a false ceiling nor PV panels (A);
2. The building has a false ceiling, but lacks PV panels (B);
3. The building has a false ceiling and a Semitransparent Photovoltaic system is integrated as the roof top (C).

The following assumptions have been made in order to write the energy balance equations:

a. A one-dimensional heat conduction is considered in the present study;
b. The system under consideration is in quasi-steady state;
c. The incident solar radiation is uniform on both sides of the roof;
d. The building is considered as one piece without internal heat source;
e. Air properties are constant with time and temperature.

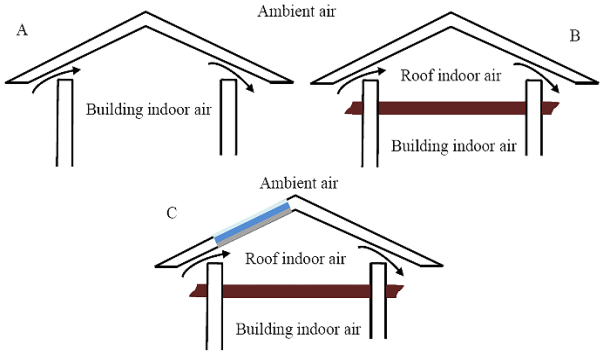

Figure 1. Pictorial view of the different cases studied, A) without BIPV system and false ceiling; B) false ceiling, without BIPV system; C) with BIPV system and ceiling false ceiling

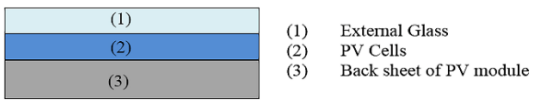

Figure 2. Pictorial view of studied BIPV module

3.1. Simple roof

Figure 1A shows a pictorial view of the building in the absence of the false ceiling and the BIPV system. Following Figure 1A, the energy balance for each component of the thermal system is:

Roof

On the outer surface of the roof, the equation expressing the energy balance is:

$$(T_s-T_r)/R_r=A_r\alpha_r I(t)+h_0A_r(T_a-T_s) \quad (1)$$

By replacing each term by its expression, we have obtained the expression of temperature on the outer surface of the roof:

$$T_s=\{T_r+R_r[A_r\alpha_r I(t)+h_0A_r]\}/[1+h_0A_rR_r] \quad (2)$$

On the inner surface of the roof, the equation expressing the energy balance is:

$$(T_s-T_r)/R_r=h_{i,roof}A_r(T_r-T_{in}) \quad (3)$$

By replacing each term by its expression, we have obtained the expression of temperature on the inner surface of the roof:

$$T_r=[T_s+T_{in}h_{i,roof}A_rR_r]/[1+h_{i,roof}A_rR_r] \quad (4)$$

The expression of the heat flux getting in the building through the roof is given by:

$$\varphi_1=(T_a-T_{in})/[(1/h_0)+(e_{al}/k_{al})+(1/h_{i,roof})] \quad (5)$$

Ambient air of the building

The energy balance equation for the ambient air in the building is given by:

$$\dot{m}_r C_{air}\frac{dT_{in}}{dt}=(T_a-T_{in})\begin{bmatrix}K_{11}+AU_0\\-0.33N_0\dot{V}+K_{12}\end{bmatrix}+h_{i,roof}A_r(T_r-T_{in}) \quad (6)$$

Upon solving Eq. (6) and applying the initial condition $T_{in}(t=0)=T_{in,\,initial}$, the building air temperature is obtained as follows:

$$T_{in}=(F_{in1}/G_{in1})+[T_{in_{initial}}-(F_{in1}/G_{in1})]\exp(-G_{in1}t) \quad (7)$$

3.2. Roof with false ceiling

Figure 1B shows a pictorial view of the building having a false ceiling in the absence of a BIPV system. The major difference between Case 3.1 and Case 3.2 is the reduction of heat transferred to the leaving space due to the presence of the false ceiling to the building. Following Figure 1B, the energy balance for each component of the thermal system is as follows:

Roof

i. On the outer surface of the roof, by applying the first principle of thermodynamics, the equation of the energy balance is the same as that in Case 3.1.

ii. On the inner surface of the roof, by applying the first principle of thermodynamics and replacing each term by its expression, we have obtained the expression of temperature on the inner surface of the roof:

$$T_r=(T_s+T_{av}h_{i,av}A_rR_r)/(1+h_{i,av}A_rR_r) \quad (8)$$

False ceiling air temperature

The energy balance equation for the ambient air in the false ceiling is given by:

$$\dot{m}_r C_{air}\frac{dT_{av}}{dt}=(T_a-T_{av})K_{21}-(T_{av}-T_{in})K_{22}+h_{i,av}A_r(T_r-T_{av}) \quad (9)$$

By integrating Eq. (9) and applying the initial condition $T_{av}(t=0)=T_{av_{initial}}$, the false ceiling air temperature is obtained as follows:

$$T_{av}=(F_{av1}/G_{av1})+[T_{av_{initial}}-(F_{av1}/G_{av1})]\exp(-G_{av1}t) \quad (10)$$

The expression of the heat flux getting in the building through the roof is given by:

$$\varphi_2=US(\Delta T)=(T_a-T_{in})\Big/\begin{Bmatrix}(1/h_0)+(e_{al}/k_{al})+(1/h_{i,av})\\+(e_{cpl}/k_{cpl})+(1/h_{i,in})\end{Bmatrix} \quad (11)$$

Ambient air of the building

The energy balance equation for the air in the building is given by:

$$\dot{m}_r c_{air}\frac{dT_{in}}{dt}=q_{wall}+q_{floor}+q_{openings}-q_{air,replenishement}+q_{false\_ceiling} \quad (12)$$

By replacing each term by its expression and applying the initial condition $T_{in}(t=0)=T_{in_{initial}}$, the building ambient air temperature is obtained as follows:

$$T_{in}=(F_{in2}/G_{in2})+[T_{in_{initial}}-(F_{in2}/G_{in2})]\exp(-G_{in2}t) \quad (13)$$

3.3. PV roof with false ceiling

Figure 1C shows a pictorial view of the building having a false ceiling and a BIPV system, while Figure 2 shows a pictorial view of the PV collector. The major difference between Case 3.3 and case 3.2 is the roof heat flux which will differ, due to the addition of the PV modules to the roof of the building. Following Figure 1C, the energy balance for each component of the thermal system is as follows:

PV module

At the glass cover of the photovoltaic module, by applying the first principle of thermodynamics, the equation of the energy balance is:

$$-\tau_g I(t)+\alpha_g I(t)+(k_g/e_g)[A_r(T_c-T_g)-h_0A_r(T_g-T_a)]=0 \quad (14)$$

By replacing each term by its expression, we have obtained the expression of temperature at the Glass cover of the photovoltaic module:

$$T_g=\begin{bmatrix} I(t)(\alpha_g-\tau_g) \\ +(k_g/e_g)T_c+h_0T_a \end{bmatrix} \Big/ \left[(e_g/k_g)+(1/h_0)\right]^{-1} \quad (15)$$

At the Solar cell of the photovoltaic module, by applying the first principle of thermodynamics, the equation of the energy balance is as follows:

$$\tau_g\alpha_c\beta_c I(t) + \tau_g\alpha_T(1-\beta_c)I(t) - \tau_g\alpha_c\beta_c\eta_c I(t) - (k_{bs}/e_{bs})(T_c-T_{bs}) - \left[(e_g/k_g)+(1/h_0)\right]^{-1}(T_c-T_a) = 0 \quad (16)$$

By replacing each term by its expression, we have obtained the expression of temperature at the Solar cell of the photovoltaic module:

$$T_c = \frac{\left[\left(\frac{e_g}{k_g}+\frac{1}{h_0}\right)^{-1}T_a+\left(\frac{e_{bs}}{k_{bs}}\right)^{-1}T_{bs}+(\tau\alpha)_{eff}\,I(t)\right]}{\left[\left(\frac{e_g}{k_g}+\frac{1}{h_0}\right)^{-1}+\left(\frac{e_{bs}}{k_{bs}}\right)^{-1}\right]} \quad (17)$$

At the Back sheet of the PV module, by applying the first principle of thermodynamics, the equation of the energy balance is:

$$h_{cbs}(T_c-T_{bs})+h_{ibsav}(T_{av}-T_{bs}) = 0 \quad (18)$$

By replacing each term by its expression, we have obtained the expression of temperature at the Back sheet of the PV module:

$$T_{bs}=(h_{cbs}T_c+h_{ibsav}T_{av})/(h_{cbs}+h_{ibsav}) \quad (19)$$

False ceiling air temperature

The energy balance equation for the air in the air gap is given by:

$$m_r c_{air}\frac{dT_{av}}{dt} = q_{wall,roof} + q_{c\text{-}i} - q_{air,interior} - q_{air,replenishement} \quad (20)$$

By proceeding similarly as in Case 4.2, the building air temperature is obtained as:

$$T_{av}=(F_{av3}/G_{av3})+\left[T_{av_{initial}}-(F_{av3}/G_{av3})\right]\exp(-G_{av3}t) \quad (21)$$

To compute the expression of the heat flux getting in the building through the roof, Figure 3 illustrates the thermal resistance of the insulation. Following Figure 3, the roof heat flux is obtained by :

$$\varphi_3 = US(\Delta T) = (T_a-T_{in})/R_{total}$$
$$R_{total} = R_{conv_{ext}} + \left\{1/\left[(1/R_{roof})+(1/R_{BIPV})\right]\right\} + R_{conv_{av}} + R_{cpl} + R_{conv_{in}} \quad (22)$$

Ambient air of the building

The energy balance equation for the air in the building is given by:

$$\dot{m}_r c_{air}\frac{dT_{in}}{dt} = q_{wall} + q_{floor} + q_{openings} - q_{air,replenishement} + q_{false\_ceiling} \quad (23)$$

By replacing each term by its expression and applying the initial condition $T_{in}(t=0)=T_{in_{initial}}$, the building ambient air temperature is obtained as follows:

$$T_{in}=(F_{in2}/G_{in2})+\left[T_{in_{initial}}-(F_{in2}/G_{in2})\right]\exp(-G_{in2}t) \quad (24)$$

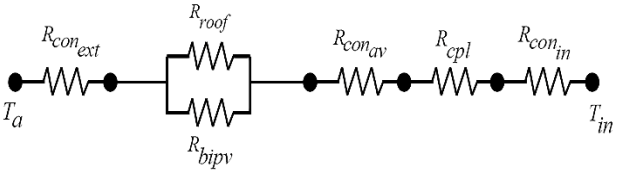

Figure 3. Thermal resistance

4. OPERATING PARAMETERS

In order to obtain the dynamic behavior of the three thermal systems and determine the ambient air temperature of the building, we used hourly global and diffuse solar radiation data over the town of Yaoundé, Cameroon for the year 2016 obtained from the Energy and Environmental Technologies Laboratory of the Department of Physics at the University of Yaoundé I. In addition, the hourly ambient temperature variation from the climatic data issued by the Atmospheric Physics Laboratory was used.

The total solar radiation over inclined roof is obtained using Eq. (25) [20]:

$$I(t)=\left[I_g(t)-I_d(t)\right]R_b+\frac{1}{2}(1+\cos\theta)I_d(t)+\frac{1}{2}(1-\cos\theta)\rho_{alb}I_g(t) \quad (1)$$

1. The equation of the energy balance on the outer surface of the roof is used to obtain the outer roof temperature. The latter is introduced in the equation of the energy balance on the inner surface of the roof in order to have the expression of the inner roof temperature as a function of the temperature of the ambient air of the building.
2. The so-obtained expression is introduced in the equation (differential) of the energy balance of the room to have an analytical expression of the indoor air temperature of the building.
3. A system of equation is therefore obtained and solved numerically with MATLAB R2016b software.
4. The same procedure is repeated for the two other thermal systems, as shown below.
5. The whole procedure is illustrated in Figure 4, including the computation of the roof heat flux.

Design specification and operating parameters of the building are presented in Table 1. These have been used as input parameters for energy analysis.

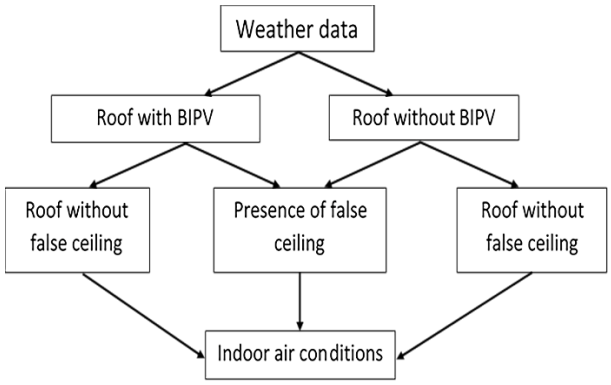

Figure 4. Flow chart of the modeling of the thermal system

Table 1. Design parameters of a building and semitransparent PV module

Parameters	Values
b	6.3 m
d	4.5 m
PV roof area	28.35 m^2
C_f	0.38
C_{air}	1005 J kg^{-1} K^{-1}
α_C	0.9
α_T	0.5
β_C	0.83
τ_g	0.9
η_C	0.12

5. RESULTS AND DISCUSSION

Figure 5 illustrates the variations of average solar radiation and ambient temperature of Yaoundé for the year 2018.

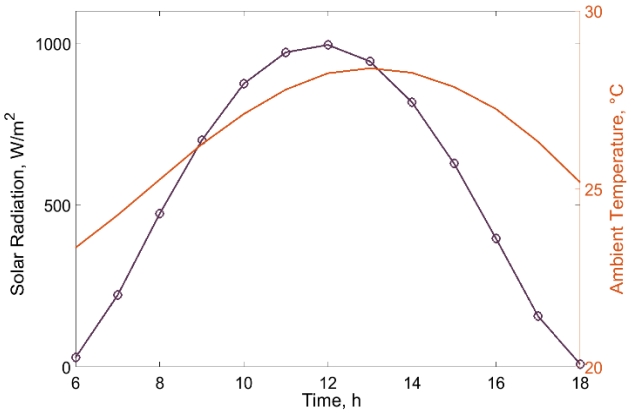

Figure 5. Average solar radiation and ambient temperature

The peak irradiation on the horizontal surface is 994.13 W/m^2 and the peak solar radiation obtained with a tilt angle of 20° South is 992.62 W/m^2. The solar radiation is maximal when the tilt angle is close from the latitude of the location under investigation. However, taking into account the building habits in the tropical climate of Cameroon, a tilt angle of 4° is rarely used for the installation of the roof. This is to avoid the labor cost and work required for cleaning the roof and the photovoltaic system of the horizontal roof. Hence, the solar radiation obtained with a tilt angle of 20° South is used in the rest of this work.

Figure 6 shows the average hourly variations of the average indoor temperature in the case of the roof only. The maximum average indoor air temperature is 30 °C around 12.00 A.M., which is 2 °C higher than the maximum average ambient temperature. This fact can be explained by the weak thermal resistance in the case of a simple roof; the roof is made only of steel; this favors a great heat absorption of heat which will be transferred to the living space.

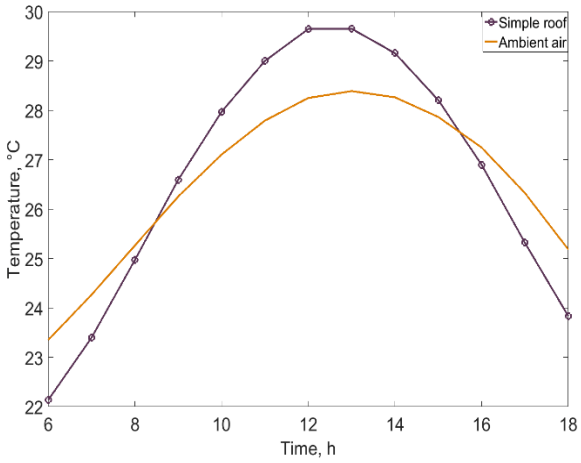

Figure 6. Average indoor air temperature of the building with a simple roof

The introduction of the false ceiling leads to a significant reduction in the room air temperature illustrated in Figure 7; the average maximum value of the indoor air temperature declines to 27.13 °C. The new indoor air temperature is almost 3 °C less than the case of simple roof. This significant temperature reduction is due to the addition of the false ceiling to the roof of the building, as this addition will increase the thermal resistance of the roof.

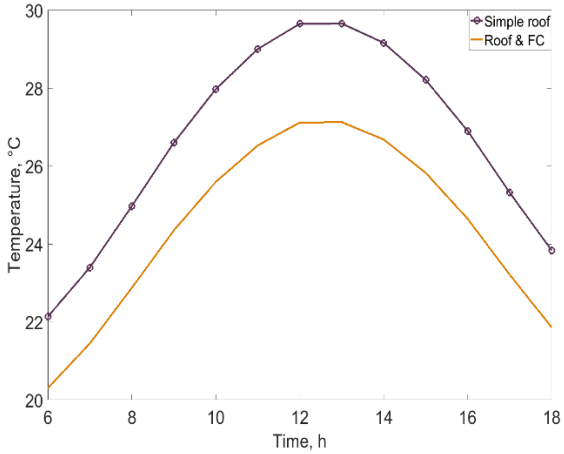

Figure 7. Average indoor air temperature of the building with Simple roof and false ceiling (FC)

The integration of the BIPV system on the roof top of the building, even though beneficial to the building because of the production of electric and thermal power, has the inconvenience of increasing the indoor air temperature of the building, as shown in Figure 8. The average air temperature of 33 °C is obtained. The difference in temperature caused by the introduction of the BIPV in the envelope of the building can be estimated to about 5 °C. Such a temperature may cause uncomfortable conditions for the occupants of the building.

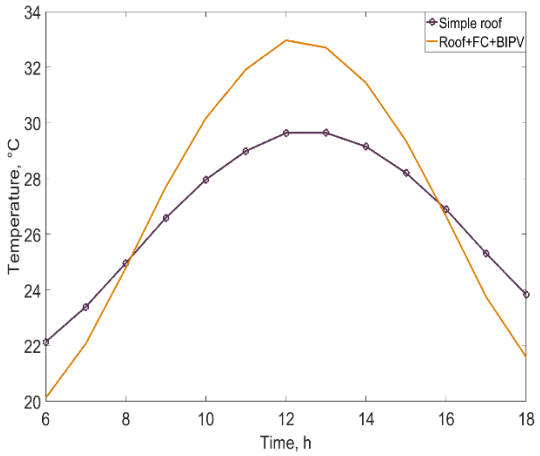

Figure 8. Average indoor air temperature of the building with roof, false ceiling, and the BIPV system

To overcome this inconvenience, a wooden layer can be placed just at the back sheet of the PV module, or the thickness of the false ceiling can be increased. The issue of placing a wooden layer just at the back sheet of the PV module is shown in Figure 9 (a). The average indoor air temperature rise due to the BIPV integration on the roof of the building has been completely reduced when the thickness of the wooden layer is equal to half that of the false ceiling and to an optimal value of 27.1 °C when the thickness of the wooden layer is equal to twice that of the false ceiling, as shown in Figure 9 (b). These results show that a great part of the heat gained by a building is distributed through the envelope of the building and especially the roof, hence succeeding in the reduction of heat transfer through the roof leads to the significant reduction of the heat exchanges between a building and its surroundings, and the consequence is a comfortable temperature of the indoor air of the building.

The results shown in Figure 9 enable us to assert that an increase in the thickness of the wooden layer just at the back sheet of the PV module leads to a greater reduction in the average indoor air temperature of the building. This assertion can be explained by the thermal inertia of building materials which plays a significant role in thermal comfort of the buildings. It is the case of materials as the wood which has weak thermal inertia and is adapted to the climatic zones where one wants to improve the thermal comfort of the interior section of the room. The increase of the wooden layer will certainly cause an increase in the weight of the framework, the latter being expected to firmly support the insulation. Hence, it is essential to correctly dimensionalize the wooden layer, taking into account the rest of the roof and the other elements of the building; this dimensioning will permit to obtain an acceptable weight of the whole framework. The use of an insulation layer placed under the roof can therefore be considered as an interesting solution to lower the indoor air temperature, thereby increasing the thermal comfort of the room in tropical climates. The insulating material is not necessarily the same and the choice of the material may vary from one location to another, but the final aim remains the same. The authors [21] recommend using 50 mm of fibreglass and foil aluminium to respectively reduce the ceiling temperature by about 3 °C and 2 °C in the tropical climate of Malaysia. However, in Cameroon, the use of wood as an insulating material is very common, hence favoring its use in the BIPV system.

The maximum average indoor air temperature of the room obtained with the addition of the wooden layer under the back sheet of the PV module is 27.1 °C, depending on the thickness of the wooden layer. The ideal interval of temperature is 23 to 26 °C in summer, and 20 to 23.5°C in winter, as recommended by the ASHRAE standards. The temperatures obtained from the modelling done in this work are slightly higher than those recommended by the ASHRAE, but these temperatures can be considered as comfortable in a tropical climate of Cameroon, where the subjects accommodate easily to such a temperature as they live in a hot climatic area, and they have adapted their bodies to temperatures greater than 27 °C without the use of an air-condition system, even though 27 °C is considered as hot by the international standards; hence, the important results obtained from our modelling can be applied to the case of Cameroon for the production of electric power using solar radiation.

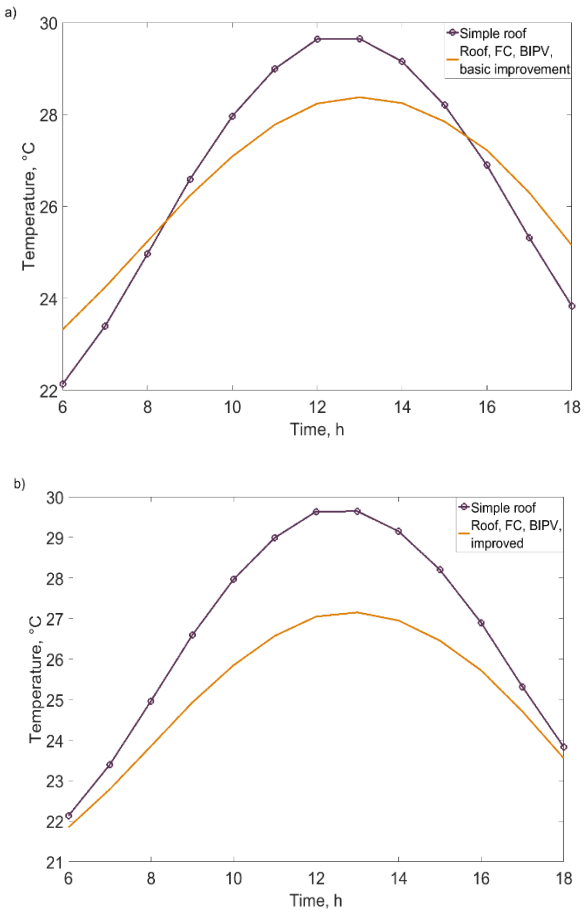

Figure 9. Average indoor temperature of the building with simple roof, false ceiling and the BIPV system when a) the thickness of the wooden layer is equal to half that of the false ceiling; b) the thickness of the wooden layer is equal to double that of the false ceiling

Figure 10 (a) shows that the indoor air temperature could be affected by an increase in the size of the BIPV surface replacing the roof of the building, while Figure 10 (b) focuses on the influence on indoor air temperature with an increase in the speed of the wind in the air in the space between roof and false ceiling in which case the space is not closed. As it can be expected, the temperature will rise if the number of PV panels increases. A quasi-regular increase is observed. The limit will be reached when the whole roof is replaced by PV panels. However, as the present study is done in the tropical climate, such a rise is not too much useful, as the produced heat cannot

be used for the heating of the indoor space. Hence, a compromise should be found between the number of PV panels to be installed and the maximum value of the indoor temperature which must not be exceeded. In Figure 10 (b), the speed of the air between roof and false ceiling has, been doubled, resulting in a significant reduction in the maximum temperature of indoor temperature. The maximum indoor temperature reached in the present case is 25.63 °C, a value almost 2 °C less than the one obtained in the previous case. Such result is logic, as an increase in the speed of the air between the roof and the false ceiling will create a fast removal of the heat stocked on the back sheet of PV panels, hence preventing heat from entering in the indoor air space. Therefore, increasing in the speed of the air between the roof and the false ceiling can greatly contribute to the reduction of the indoor air temperature caused by an increase in the size of the BIPV system, thereby improving the thermal comfort of the occupants of the building.

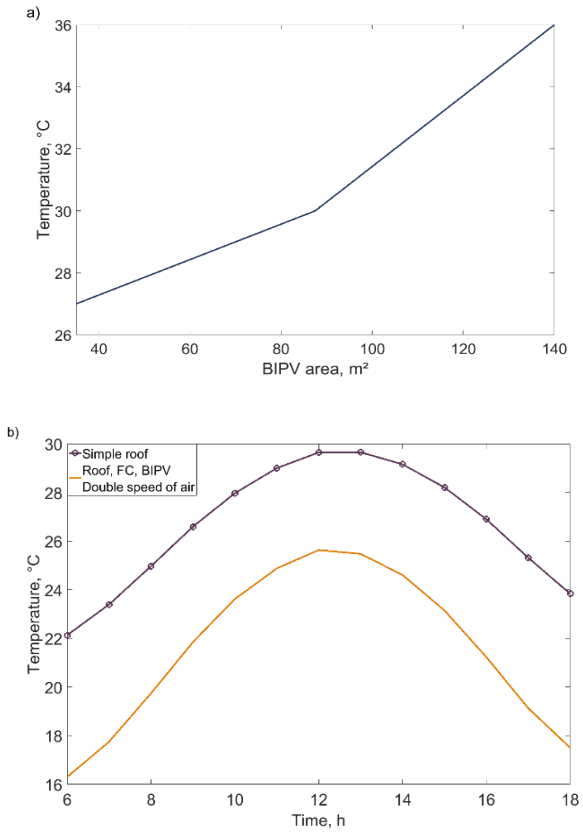

Figure 10. Average indoor temperature of the building with roof, false ceiling and the BIPV system when (a) the size of the BIPV system is increased; (b) the speed of the air in the dead space is doubled

Figure 11 illustrates the roof heat flux of the building for the different cases studied in the modelling. It can be observed that the highest values of heat flux are obtained when the BIPV system is added to the roof and the false ceiling, followed the case of the simple roof. The use of the wooden layer just under the PV modules greatly reduces the roof heat flux, hence showing the positive effects on the indoor comfort conditions of the wooden layer placed just under the PV panels. Another observation that can be made from Figure 11 is that the roof heat flux is maximal during the period comprised between 10 a.m. and 4 P.M.; this observation can be explained by the fact that the highest values of temperatures are obtained during the noon and the afternoon, and the accumulated effect of the irradiation absorbed since the morning will have the overall effect of lowering the thermal resistance of the envelope elements. The results obtained clearly show that the maximum heat transfer in a residential building is done through the roof of the building. The roof heat flux in case of the simple roof is maximum at noon, as it reaches 250 W/m^2, a value almost 8 times greater than the heat flux density through the walls (29 W/m^2 in Yaoundé, 38 W/m^2 in Garoua from the authors of [22]). This value declines to 155.77 W/m^2, thanks to the use of the false ceiling. Introducing PV panels to the roof increases the roof heat flux, with a maximum value of 300 W/m^2, but an appropriate use of the false ceiling brings back the heat flux to a value of 169 W/m^2 and to 132 W/m^2 with the increase of the wooden layer placed just under the PV module. Therefore, reducing indoor temperature can lead to a reduction in the roof heat flux, hence the improvement of the thermal comfort of the occupants of the building. These results are in accordance with previous studies [23] and show all the benefits of an appropriate use of local building materials to increase the indoor comfort of buildings.

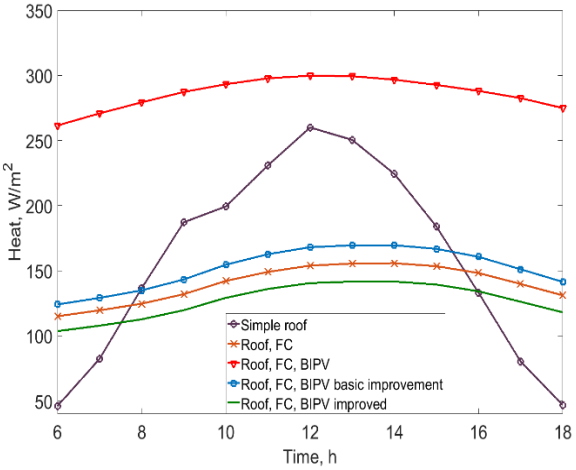

Figure 11. Heat transfer through the roof to the leaving space in the five (05) cases studied

The heat transfer model for the indoor air temperature of the building is simplistic, as the results of this modelling were obtained by considering the entire building as a unique piece without internal heat source. The different temperatures of each room of the building have not been studied, whereas such a study could have improved the degree of precision of the modelling. Taking into account the heat generated by the occupants and the devices of the building would certainly lead to an increase in the temperature of the indoor air of the building. In addition, the heat loss due to ventilation (mechanical or natural) of the building is not sufficiently taken into account in the model. Another factor to consider is that the heat transfer through radiation should be more considered in the elaboration of the modelling, as radiation occupies an important place in the heat exchanges between the building and its environment, especially those taking place through the roof of the building. Also, means must be implemented to reduce the temperature of the PV cells, e.g., adding fins at the back of the PV module, or increasing the natural ventilation around the PV module. This ventilation may be done by creating small adjustable openings around building envelope just under the ceiling or making an open roof-ceiling system.

6. CONCLUSIONS

We presented three distinct but related concepts: first, the irradiation on a tilted surface; second, the lowering of the indoor temperature variation; last, the reduction of the roof heat transfer. The thermal analysis of each of the three systems, the first one consisting of a building without a false ceiling and a BIPV system, the second one consisting of a building with a false ceiling in the absence of a BIPV system, and the third one consisting of a building with a false ceiling and a BIPV system on which a wooden layer is later added just under the back sheet of the PV module was conducted. This study allowed us to demonstrate that:

1. Taking into account the building customs of Cameroon, a tilt angle of 20°S, can be adopted as the tilt angle of the solar roof of our modeling.
2. The building with a roof only had a high room air temperature, approximately 30 °C. The roof heat flux in case of the roof only reaches a maximum of 250 W/m^2, but the use of a false ceiling lowers the density flux to 169 W/m^2.
3. The introduction of the false ceiling lowers the indoor temperature by about 2.5 °C.
4. The association between the false ceiling and a BIPV system makes the room air temperature rise to approximately 32.5 °C.
5. The addition of a wooden layer just under the back sheet of the PV module brings back the room air temperature to 27.71 °C, when the thickness of the wooden layer is equal to twice that of the false ceiling.
6. The increased area of the BIPV system yields an increase in the indoor air temperature; the latter increase can be reduced by increasing the speed of air located in the dead space.
7. The addition of the PV brings back the roof heat flux to the rise, about 300 W/m^2, but this value can be greatly reduced by the appropriate use of the false ceiling and the natural ventilation (134 W/m^2).
8. The reduction of the indoor temperature and the roof heat flux increase the thermal comfort of the occupants of the building.
9. As the wood is considered to be among the building local materials, we recommend its use for the optimization of thermal insulation between the roof system and the floor supporting that roof.

The practice of optimizing the building envelope through the thermal insulation of this envelope should be required either in the construction of new buildings or the renovations of already existing buildings in Cameroon. The use of a well-planned false ceiling makes the solar roof more attractive in a tropical region of Africa.

7. ACKNOWLEDGEMENT

The research was carried out and supported by the corresponding author's grant.

NOMENCLATURE

A	Area (m^2)
b	Height of the BISPVT system (m)
C	Specific heat (J/kg K)
C_f	The conversion factor of the thermal power plant
d	Width of the BISPVT system (m)
dx	Elemental length (m)
dt	Elemental time (s)
e	Thickness (m)
h	Heat transfer coefficient (W/m^{2}K)
k	Thermal conductivity (W/mK)
L	Length (m)
$\dot{m}$	Mass flow rate (kg/s)
R	Thermal resistance (K/W)
T	Temperature (K)
t	Time (s)
I(t)	Incident solar radiation (W/m^2)
U	Overall heat transfer coefficient (W/m^{2}K)
$(UA)_t$	Overall heat transfer coefficient from room to ambient air (W/K)
V	Volume (m^2), Velocity (m/s)
Greek letters	
α	Absorptivity
β	Packing factor, Volume expansion Coefficient
θ	Inclination of roof (rad)
τ	Transmissivity
η	Efficiency
$(\alpha\tau)_{eff}$	Product of effective absorptivity and transmittivity
ρ_{alb}	Albedo
ϑ	Viscosity
φ	Heat flux (W/m^2)
Subscripts	
a	Ambient
al	Aluminum
av	Air in the gap
bs	Back sheet of PV
c	PV cell
door	Door
Fc	False ceiling
g	Glass cover of PV
i	Inner surface
in	Indoor air of the building
n	Number
o	Outer surface
r	Roof
s	Roof exterior surface
T	Tedlar

APPENDIX

$$G_{in1}=\frac{1}{\dot{m}_r c_{air}}\begin{bmatrix}K_{11}+K_{12}+AU_0\\ -0.33N_0\dot{V}+h_{i,roof}A_r\end{bmatrix}$$

$$F_{in1}=\frac{1}{\dot{m}_r c_{air}}\left\{T_a\begin{bmatrix}K_{11}+K_{12}\\ +AU_0-0.33N_0\dot{V}\end{bmatrix}+T_r h_{i,roof}A_r\right\}$$

$$G_{in1}=\frac{1}{\dot{m}_r c_{air}}\begin{bmatrix}K_{11}+K_{12}+AU_0\\ -0.33N_0\dot{V}+h_{i,roof}A_r\end{bmatrix}$$

$$F_{in1}=\frac{1}{\dot{m}_r c_{air}}\left\{T_a\begin{bmatrix}K_{11}+K_{12}\\ +AU_0-0.33N_0\dot{V}\end{bmatrix}+T_r h_{i,roof}A_r\right\}$$

$$G_{av1}=\frac{1}{\dot{m}_r c_{air}}\begin{bmatrix}K_{21}-0.33N_0\dot{V}\\ +K_{22}+h_{i,av}A_r\end{bmatrix}$$

$$F_{av1}=\frac{1}{\dot{m}_r c_{air}}\left\{\begin{matrix}T_a\left[K_{21}-0.33N_0\dot{V}\right]\\ +K_{22}T_{in}+h_{i,av}A_r T_r\end{matrix}\right\}$$

$$G_{in2}=\frac{1}{\dot{m}_r c_{air}}\begin{bmatrix}K_{22}+K_{23}+K_{24}\\+AU_0-0.33N_0\dot{V}\end{bmatrix}$$

$$F_{in2}=\frac{1}{\dot{m}_{fc} c_{air}}\left\{\begin{bmatrix}T_a\begin{bmatrix}K_{23}+K_{24}\\-0.33N_0\dot{V}+AU_0\end{bmatrix}\\+K_{22}T_{av}\end{bmatrix}\right\}$$

$$G_{av3}=\frac{1}{\dot{m}_{fc} c_{air}}\begin{bmatrix}K_{31}-0.33N_0\dot{V}\\+K_{32}+h_{ibsav}A_r\end{bmatrix}$$

$$F_{av3}=\frac{1}{\dot{m}_{fc} c_{air}}\left\{\begin{bmatrix}T_a\left[K_{31}-0.33N_0\dot{V}\right]T_{in}K_{32}\\+h_{ibsav}A_r T_{bs}\end{bmatrix}\right\}$$

$$K_{21}=K_{31}=\left(\begin{bmatrix}\frac{1}{h_0 A_{wall}}+\frac{e_{wall}}{k_{wall}A_{wall}}\\+\frac{1}{h_{i,wall\_fc}A_{wall}}\end{bmatrix}\right)^{-1}$$

$$K_{22}=K_{32}=\left(\begin{bmatrix}\frac{1}{h_{i,av}A_{fc}}+\frac{e_{plywood}}{k_{plywood}A_{fc}}\\+\frac{1}{h_{i,in}A_{fc}}\end{bmatrix}\right)^{-1}$$

$$K_{11}=\left(\frac{1}{h_0 A_{wall}}+\frac{e_{wall}}{k_{wall}A_{wall}}+\frac{1}{h_{i,wall}A_{wall}}\right)^{-1}$$

$$K_{12}=\left(\begin{bmatrix}\frac{1}{h_0}\left[\frac{1}{A_{door}}+\frac{1}{A_{wd}}\right]+\frac{e_{door}}{k_{door}A_{door}}\\+\frac{e_{wd}}{k_{wd}A_{wd}}+\frac{1}{h_{i,door}A_{door}}+\frac{1}{h_{i,wd}A_{wd}}\end{bmatrix}\right)^{-1}$$

REFERENCES

1. Ang, B.W. and Xu, X., "Energy efficiency indicator", Encyclopedia of quality of life and well-being research, Michalos, A.C. Ed., Vol. 7, Springer, Dordrecht, (2014), 1894-1897. (https://doi.org/10.1007/978-94-007-0753-5_875).
2. Stouter, P., Earthbag building in the humid tropics : Simple structures, (2011). (http://www.earthbagbuilding.com/pdf/earthbagbuilding2.pdf), (Accessed: 05 September 2020).
3. Chen, H.-J., Shu, C.-M., Chiang, C.-M. and Lee, S.-K., "The indoor thermal research of the HCRI-BIPV smart window", ***Energy Procedia***, Vol. 12, (2011), 593-600. (https://doi.org/10.1016/j.egypro.2011.10.080).
4. Akwa, J.V., Konrad, O., Kaufmann, G.V. and Machado, C.A., "Evaluation of the photovoltaic generation potential and real-time analysis of the photovoltaic panel operation on a building facade in southern Brazil", ***Energy and Buildings***, Vol. 69, (2014), 462-433. (https://doi.org/10.1016/j.enbuild.2013.11.007).
5. James, T., Goodrich, A., Woodhouse, M., Margolis, R. and Ong, S., "Building-integrated photovoltaics (BIPV) in the residential sector: An analysis of installed rooftop system prices", ***National Renewable Energy Laboratory***, Technical Report, NREL/TP-6A20-53103, (2011). (https://www.nrel.gov/docs/fy12osti/53103.pdf).
6. Kalogirou, S.A. and Tripanagnostopoulos, Y., "Hybrid PV/T solar systems for domestic hot water and electricity production", ***Energy Conversion and Management***, Vol. 47, (2006), 3368-3382. (https://doi.org/10.1016/j.enconman.2006.01.012).
7. Chow, T.T., He, W. and Ji, J., "Hybrid photovoltaic-thermosyphon water heating system for residential application", ***Solar Energy***, Vol. 80, (2006), 298-306. (https://doi.org/10.1016/j.solener.2005.02.003).
8. Ekoe A Akata, A.M., Njomo, D. and Agrawal, B., "Thermal energy optimization of building integrated semi-transparent photovoltaic thermal systems", ***International Journal of Renewable Energy Development (IJRED)***, Vol. 4, No. 2, (2015), 113-123. (https://doi.org/10.14710/ijred.4.2.113-123).
9. Maturi, L., Lollini, R., Moser, D. and Sparber, W., "Experimental investigation of a low cost passive strategy to improve the performance of building integrated photovoltaic systems", ***Solar Energy***, Vol. 111, (2015), 288-296. (https://doi.org/10.1016/j.solener.2014.11.001).
10. Chow, T.T., He, W., Ji, J. and Chan, A.L.S., "Performance evaluation of photovoltaic thermosyphon system for subtropical climate application", ***Solar Energy***, Vol. 81, (2007), 123-130. (https://doi.org/10.1016/j.solener.2006.05.005).
11. Pierrick, H., Christophe, M., Leon, G. and Patrick, D., "Dynamic numerical model of a high efficiency PV-T collector integrated into a domestic hot water system", ***Solar Energy***, Vol. 111, (2015), 68-81. (https://doi.org/10.1016/j.solener.2014.10.031).
12. Rawat, P., Debbarma, M., Mehrotra, S., Sudhakar, K., Centre, E. and Pradesh, M., "Design, development and experimental investigation of solar photovoltaic/thermal (PV/T) water collector system", ***International Journal of Science, Environment and Technology***, Vol. 3, No. 3, (2014), 1173-1183. (https://www.researchgate.net/publication/263448257_DESIGN_DEVELOPMENT_AND_EXPERIMENTAL_INVESTIGATION_OF_SOLAR_PHOTOVOLTAICTHERMAL_PVT_WATER_COLLECTOR_SYSTEM).
13. Benradouane, N., "Performances thermiques d'une maison solaire", ***Rev. Energ. Ren.***, Vol. 9, (2006), 43-52. (https://www.cder.dz/download/Art9-1_6.pdf).
14. Obeng, G.Y., Akuffo, F.O., Braimah, I., Evers, H.-D. and Mensah, E., "Impact of solar photovoltaic lighting on indoor air smoke in off-grid rural Ghana", ***Energy for Sustainable Development***, Vol. 12, (2008), 55-61. (https://doi.org/10.1016/S0973-0826(08)60419-6).
15. López, C.S.P., Tenconi, L., Castro, F. L., Brambillasca, S., Gonzalez, F.J.N., and Martín, E.C., "Controlled environment test laboratory for comfort performance studies on façade-integrated BIPV", ***Proceedings of the 27th European Photovoltaic Solar Energy Conference and Exhibition***, (2012), 4335-4339. (https://doi.org/10.4229/27thEUPVSEC2012-5BV.1.57).
16. Wen, I.J., Chang, P.C., Chiang, C.M. and Lai, C.M., "Performance assessment of ventilated BIPV roofs collocating with outdoor and indoor openings", ***Journal of Applied Sciences***, Vol. 8, (2008), 3572-3582. (https://doi.org/10.3923/jas.2008.3572.3582).
17. Dominguez, A., Kleissl, J. and Luvall, J.C., "Effects of solar photovoltaic panels on roof heat transfer", ***Solar Energy***, Vol. 85, (2011), 2244-2255. (https://doi.org/10.1016/j.solener.2011.06.010).
18. Ekoe a Akata, A.M., Njomo, D., and Mempouo, B., "The effect of building integrated photovoltaic system (BIPVs) on indoor air temperatures and humidity (Iath) in the tropical region of Cameroon", ***Future Cities and Environment***, Vol. 1, (2015), 1-10. (https://doi.org/10.1186/s40984-015-0002-y).
19. Ali, H.A.R., Ibrahim, S.T., Morsy, M.G. and Abdel-Rahman, A.K., "The effect of using false ceiling on roof cooling load", ***Journal of Engineering Sciences***, Vol. 42, No. 3, (2014), 666-682. (https://doi.org/10.21608/JESAUN.2014.115021).
20. Duffie, J.A. and Beckman, W.A., Solar engineering of thermal processes, Fourth Edition, Wiley, (2013). (https://doi.org/10.1002/9781118671603).
21. Harimi, M., Harimi, D., Kurian, V.J. and Nurmin, B., "Evaluation of the thermal performance of metal roofing under tropical climatic conditions", ***Proceedings of The 2005 World Sustainable Building Conference***, Tokyo, (2005). 709-716. (https://www.irbnet.de/daten/iconda/CIB3434.pdf).
22. Kameni Nematchoua, M., Ricciardi, P., Reiter, S. and Yvon, A., "A comparative study on optimum insulation thickness of walls and energy savings in equatorial and tropical climate", ***International Journal of Sustainable Built Environment***, Vol. 6, (2017), 170-182. (https://doi.org/10.1016/j.ijsbe.2017.02.001).
23. Ekoe A Akata, A.M., Njomo, D. and Agrawal, B., "Assessment of Building Integrated Photovoltaic (BIPV) for sustainable energy performance in tropical regions of Cameroon", ***Renewable and Sustainable Energy Reviews***, Vol. 80, (2017), 1138-1152. (https://doi.org/10.1016/j.rser.2017.05.155).